Periodica Polytechnica
Civil Engineering

61(1), pp. 88–97, 2017
DOI: 10.3311/PPci.8836

RESEARCH ARTICLE

The Analysis of Bearing Capacity of Axially Compressed Cold Formed Steel Members

Miroslav Bešević[1*], Aleksandar Prokić[1], Aleksandar Landović[1], Karolj Kasaš[1]

Received 23-11-2015; revised 18-04-2016; accepted 17-05-2016

Abstract
This paper presents a calculation method for axially compressed cold formed stainless, high strength and carbon steel profiles. Results of different authors in this field published in international journals depict current trends in this field. Paper also presents author's numerical and experimental analysis of cold-formed centrally compressed elements. Numerical analysis was carried out by finite element method and program for the nonlinear static and dynamic structural analysis - PAK. The results obtained by experimental and numerical methods included boundary conditions, maximum force, buckling curve etc. Small difference observed in the values obtained by these different methods. Results werw compared to values predicted by international designing code in order to analyze if they are too conservative for cold formed steel sections.

Keywords
axially compressed members, experimental analysis, numerical analysis, cold formed profiles, stainless high strength steel profiles

[1]Faculty of Civil Engineering Subotica, Subotica, University of Novi Sad, Serbia
[*]Corresponding author, e-mail: miroslav.besevic@gmail.com

1 Introduction

Group of authors made series of experiments on cold formed steel sections where is shown that geometrical imperfections significantly effect on bearing capacity of the elements. Same conclusion has been made for carbon steel elements. We have to consider those factors during designing cold formed steel elements. Having that on mind we have made numerical and experimental analysis of cold-formed centrally compressed elements aspiring to show more accurate method of calculation.

Experiments have been made on five series, each containing six samples with different slenderness. Cold-formed steel (CFS) members are created by the working of sheet steel using stamping, rolling, or presses to deform the sheet into a usable product, at room temperature. This production technology effect on mechanical characteristics of the elements. We have presented the results of the effect of production technology on mechanical characteristics of rolling steel mean values in the summary diagram. In corners, changes are most pronounced and yield points are between 560-606 MPa, and on the straight parts of the profile the same value is 302 - 320 MPa.

The strength of elements used for design is usually governed by buckling. Cold-formed steel sections tend to be more sensitive to local buckling effects than typical hot rolled sections. Cross sections are generally stiffened to improve resistance to local buckling.

Results gain from experiments and with numerical analysis are compared to European buckling curves showing that they are to conservative for cold formed steel sections.

1.1 Results obtained by different authors

Narayanan and Mahendran [1] in their research showed that columns made of cold formed profiles are very sensitive to the geometric imperfection. Investigation made by Ellobady and Young [2] showed that similar conclusion can be made for stainless steel. That shows importance of including geometric imperfection into design procedure. Design rules for cold-formed stainless steel structural members includes the American Society of Civil Engineers (ASCE) Specification for the Design of Cold-Formed Stainless Steel Structural

Members [3], the Australian/New Zealand Standard (Aust/NZS) for Cold-Formed Stainless Steel Structures [4] and the European Code - Design of Steel Structures [5, 6, 7]. For column design, the design rules in the specifications are mainly based on experiment on pin-ended columns. In practice, there is some degree of deviation comparing to test specimens. Gao et al. [8] studied the load-carrying capacity of thin-walled box-section stub columns fabricated by high strength steel 18Mn2CrMoBA. Cross-sections of steel columns are presented on Fig. 1. Table 1 show base sheet thickness and nominal yield limit. Steel columns were placed in the press and loaded until failure. Results, obtained in uniaxial compression experiments on geometrically different specimens, compared with predicted values by the AISI Code.

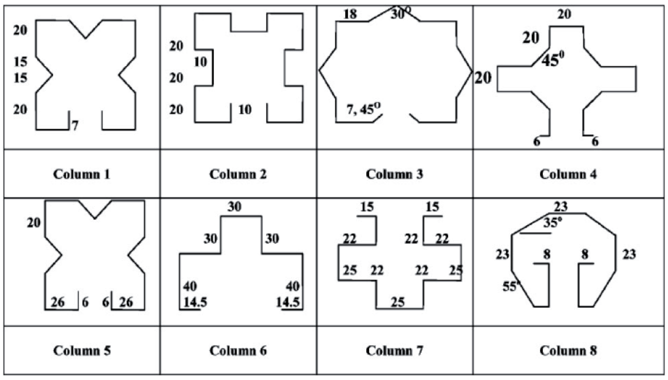

Fig. 1 Cross section shapes of cold formed profiles for tested columns

Table 1 Steel classes, base sheet thickness and yield limit

grade	base metal thickness (mm)	yield stress (MPa)
G550	0.80	656
	0.95	637
G250	0.96	326
	1.14	310

In that comparison load-carrying capacity of the high strength thin-walled box-section stub columns are much larger than predicted one, because design method suggested by the AISI Code is too conservative for this stub columns type. Young and Lui [9] also investigated high strength steel members. The test strengths compared with design strengths predicted by international codes for cold-formed high strength stainless steel columns. This research shows that design strengths predicted by the three specifications are conservative for the cold-formed high strength stainless steel columns. In addition, reliability analysis performed to evaluate the current design rules. Elbody [10] in his own investigations used same international design codes for stainless steel. The main objective of his work was to investigate behavior of cold-formed high strength stainless steel stiffened and unstiffened slender square and rectangular hollow section columns. He has used the finite element program ABAQUS in the analysis. A parametric study performed to investigate the effect of cross-section geometries on the strength and behavior of cold formed high strength stainless steel stiffened and unstiffened slender hollow section columns. The results obtained from the finite element model were compared with design strengths calculated using the international codes [3-7] for cold formed stainless steel structures. Results show that these codes, defined based on quasi-static tests, remain applicable when the buckling force is applied in cycles of small amplitudes, which typically occurs during seismic loading [11].

Young and Liu [12] described test program on cold-formed stainless steel square hollow section subjected to pure axial compression. The specimens were cold-rolled from stainless steel sheets with square (SHS) and rectangular (RHS) cross section. The tests were performed over a range of column lengths, including local buckling and overall flexural buckling. Investigation included measurements of overall geometric imperfections and material properties of the specimens. The experimental column strengths compared with the design strengths predicted by the international codes for cold formed stainless steel structures. Cold working production technology produces considerable enhancement of the material properties of the annealed steel. More economic design can be achieved by taking into account the enhancement of the material properties due to cold working. Young and Liu consider the design strengths calculated based on the material properties obtained from the finished specimens and determined the material properties by tensile coupon tests as well as stub column tests. Deflection curve is obtained for each series of test column. Movable upper support used to make tests on columns of various heights. Flexural buckling is observed in all samples of SHS1 series, except for the shortest samples in which failure occurred by material yielding. Pure local buckling has been observed in samples with an effective length less than or equal to 700 mm (le=700 mm). The interaction of local and global bending buckling observed in samples of effective length greater than or equal to 1100 mm. Detail account of measurements as well as the value and distribution of residual stresses are presented in the Young and Lui paper work [13].

Tables 2 and 3 show experimental limits σ_{02}, f_u and E_0 obtained from tensile coupons and compression tests on short columns. Numerical strength limits were determined by using the average measured cross-sectional dimensions and measured material properties according to Tables 2 and 3. For suitable stress strenght was used 0.2% σ_{o2} stress.

Table 2 Measured material properties obtained from tensile from coupon tests

Test series	Section *DxBxt* (mm)	$\sigma_{0.2}$ (MPa)	f_u (MPa)	E_0 (Gpa)	n
SHS1	40x40x2	707	827	216	4
SHS2	50x50x1.5	622	770	200	5
RHS1	140x80x3	486	736	212	6
RHS2	160x80x3	536	766	208	5

Table 3 Results of column stub tests

Test series	Section *DxBxt* (mm)	$\sigma_{0.2}$ (MPa)	f_u (MPa)	E_0 (Gpa)	n
SHS1	40x40x2	757	854	226	3
SHS2	50x50x1.5	608	618	200	4
RHS1	140x80x3	441	444	214	6
RHS2	160x80x3	390	411	213	9

Author of this paper obtained comparable results for carbon steel. All initial geometric imperfections were measured before testing.

Goggins et al. [14] investigated columns with square and rectangular cross-section. Obtained results (Table 4) shows that that American, AS /NSZ and European codes are conservative for slender columns of hollow square cross-section, except for the column lengths from 500 to 3000mm SHS.

Among others, Cruise and Gardner also investigated columns with square and rectangular cross-section [15, 16].

Table 4 Mean yield strengths of short columns

Section size (mm)	Coupon test results (MPa)	EC3 model, f_{ya} (MPa)	Tensile test results (MPa)	Tensile test/ coupon test
40 x 40 x 2.5 SHS	343.0	378.2	418.6	1.23
20 x 20 x 2.0 SHS	299.6	314.5	303.7	1.01
50 x 25 x 2.5 RHS	285.0	310.3	328.1	1.15

The average value of the initial buckling load (F_{exp}) observed in all combinations of size and member's length is shown in Table 5.

Results compared to no factorized computed forces from (FBS) standards, (Faisc) and (Fec3) standards for the dimensioning of steel structures-value force FBS, Faisc and FEC-b were calculated using material properties obtained from testing the tensile coupons. Additionally, samples with height of 1100 mm had values of force FEC-c calculated using the yield strength obtained by testing the entire section in conjunction with the European buckling curve (C). Values of force Fec-b based on buckling curve (B). For behavior simulation of cold formed high strength steel columns they used FEM software ABAQUS. Residual stresses were included in the simulation as average values for flat regions and for corner regions. Verification of the numerical model conducted on a 22 cold formed stainless steel columns and included comparison of experimental and numerical results.

In experiments on stainless steel hollow sections Gardner and Nethercot [17] specially treated basic material stress–strain curve as one particular feature of stainless steel that differs from carbon steels. Studies of the stainless steel behavior demonstrate that the material possesses a rounded stress–strain curve, with no sharp yield point. Stub column tests carried out on hollow sections (SHS, RHS) with idea to provide relationships between applied load and deformation capacity in the form of load– end shortening curves. These were then used to develop an explicit relationship between deformation capacity and cross-sectional slenderness, including an allowance for restraint to the most critical plate element from the surrounding components. The stress–strain properties of the corner regions in cold-formed stainless steel cross-sections differ from the properties of the flat regions due to the material's response to deformation. Due to the very pronounced degree of strain hardening that stainless steel exhibits, the cold-worked corner regions of cold-formed stainless steel SHS and RHS have 0.2% proof strengths commonly between 20 % and 100% higher than the 0.2 % proof strengths of the flat regions. This is accompanied by a corresponding loss in ductility. Cruise and Gardner continued with the research of changes in cold formed steel structures. As we know the material properties of stainless steel are sensitive to plastic deformation that causes an increase in yield strength by a process termed cold working. The different strain paths experienced around cold-formed cross sections

Table 5 Initial buckling loads

Section size (mm)	Specimen length (mm)	Initial buckling loads				
		$F_{exp(KN)}$	F_{BS} / F_{exp}	F_{AISC} / F_{exp}	$F_{EC3\text{-}b} / F_{exp}$	$F_{EC3\text{-}C} / F_{exp}$
40x40x2.5	1100	105.5	0.82	0.82	0.82	1.01
20x20x2.0	1100	29.5	0.94	0.93	0.92	0.84
50x25x2.5	1100	83.7	0.95	0.93	0.93	1.02
40x40x2.5	3300	52.3	0.93	0.94	0.92	-
20x20x2.0	3300	5.7	0.91	0.75	0.91	-
50x25x2.5	3300	17.2	1.25	1.15	1.28	-

during manufacture create unique material strength distributions for sections from different forming routes and influence residual stress patterns. In their research, they have examined experimentally the material and residual stress distributions in two types of cold-formed sections–cold-rolled box sections and press-braked angles. Strength enhancements induced during the forming routes of cold-formed sections, which are the most common type of stainless steel cross section, offer higher material strength than that currently assumed in design. Based on an experimental program comprising tensile coupon tests and hardness tests, a method for predicting the distribution of 0.2% proof stress around press-braked and cold-rolled stainless steel sections proposed. Due to cold working during forming strength increases beyond the material strength of the sheet material, observed in the corner regions and in the flat faces of the tested member. In experiments, regions with corner strength enhancements were defined. New models proposed to predict the strength enhancements in the faces of the cold-rolled box sections, and existing models modified in aim to predict the corner strength enhancements. Models assessed in combination with current structural design guidance, to demonstrate the increases in design efficiency. The magnitude and distribution of residual stresses in cold-formed stainless steel sections has been quantified, but wasn't take as a factor that significantly affect structural behavior. The achieved enhancements in efficiency are significant and highlight the importance and benefit of harnessing the strength increases that arise during forming of cold-formed stainless steel members.

2 Carbon steel

Design of axially compressed complex member made from cold formed profiles is a function of many parameters that affects its global and local stability. This paper gives analysis of parameters related to structural changes that occurs because of cold forming production technology. Tensile coupons, obtained from basic sheet and from finished profile, tested in order to determine tensile properties of steel: yield point (f_{yl}), tensile strength (f_u), elongation percentage (A) and Young's modulus (E). The first part of investigations deals with the increase of mechanical characteristics, particularly strain hardening, of cold formed profiles while second deals with determination of compressive yield limit, namely resistance of the section for compression, for stub column tests. Those analyses used for definition of input mechanical parameters and geometrical imperfections for calculation appropriate buckling curves for axially compressed complex steel columns made from cold formed profiles. The results of the effect of production technology on mechanical characteristics of rolling steel mean values presented in the summary diagram (Fig. 2) [18]. In corners, changes are most pronounced and yield points are between 560-606 MPa, and on the straight parts of the profile the same value is 302 - 320 MPa.

2.1 Determination of geometrical imperfections of samples

Necessary input data involved: sample geometry, initial deflection, tensile, compression tests, and the state of stress distribution. Determination of profile geometry is necessary to obtain accurate data such as : thickness, area, bend radius and static inertia moments. Deviations in the geometry of the section and whole element/sample are a consequence of cold forming production technology. Initial curvature of a sample could be notable if residual stress isn't predominant stress in element. Start imperfections dominantly affect on bearing capacity of pressed rod in case of thinner sheet-metals, because they cause additional moment of inertia as a result of normal force and initial eccentricity. Pressed rod could faster lose his capacity if start realise is larger than ordinary. Experiments were conducted on complex element, consisting of two C90x45x20x2.5 mm profiles shown on Fig. 3 [19].

2.2 Residual stresses

Residual stresses have important role in calculation of structural steel elements. Structural steel residual stress is caused by uneven cooling of cross section after hot rolling and production procedures (cold forming, pressing, welding, torch cutting, etc). In cold formed profiles, residual stress is usually caused by the effects of cold bending during forming or pressing procedures [19]. Due to production differences in two types of profiles, residual stresses in cold formed profiles can be significantly different compared to the ones in hot rolled profiles.

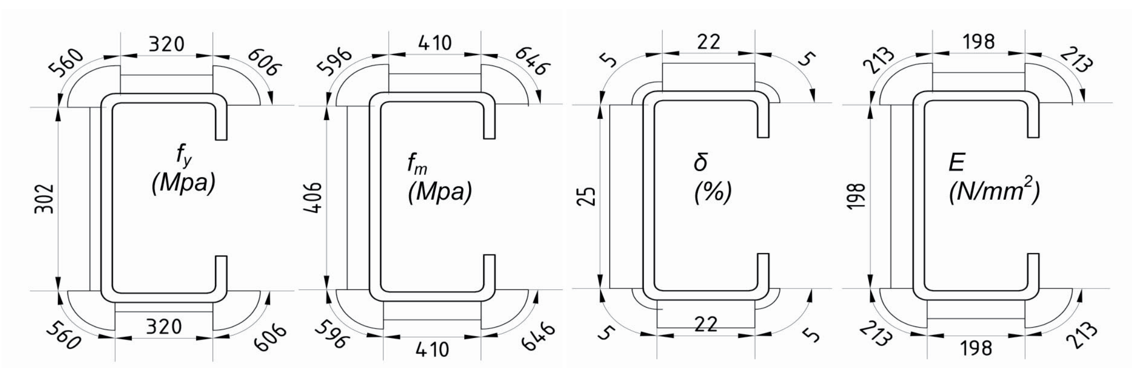

Fig. 2 Summary diagram - Mechanical characteristics of steel

When compared to stresses from working loads, effects of residual stresses can be harmful or beneficial depending on their magnitude, orientation and distribution. Often, residual stresses are harmful and there are instances when these stresses were the determining factor that contributed to fatigue or other structural failures. Analysis shown in this paper also includes residual stress distribution along the wall thickness of cold formed stainless profiles with box cross section that are currently widely used [20] and [21].

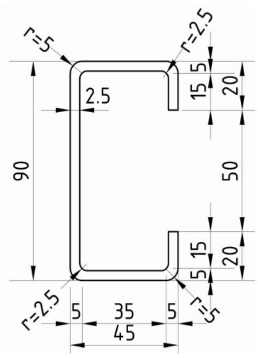

Fig. 3 Cross section of profile C90x45x20x2.5 (mm)

2.3 Initial imperfections

Measurements of initial curvature (straightness) were performed by leveling instrument Ni 0.02 ,with precision of 0.2 mm on 1000 mm. Measurement performed in a laboratory on a short (3.5 m) basis. Readings obtained by optical micrometer with precision of 1 /1000 mm + / - 5 / 100. Compensator insured verticality of α = 0.1". Measurement technique required a micrometer screw connected to the perfectly horizontal plate that enables 5 mm movements in a vertical plane. Readings were obtained along the length of a profile so that shorter samples had 5 measurement points, middle size samples 9, longer samples 13 and longest samples had 17 measurement points both for x and y direction.

3 Preparation, testing and analysis of carbon steel specimens

Axially compressed member is the one with loads that act through the centroid of the member along the longitudinal length of the member. This kind of member should not have any lateral deflection for loads less then critical, but that is for theoretical/perfect model of axially compressed member. In real time we have lateral deflections with beginning of loads act, due to the initial curvature of member and eccentricity of the applied load. This can significantly reduce load bearing limit of the member. Axially compressed built up members were tested according to European convention for obtaining the stress - strain curve with constant increase in force of 10 N/mm2 per minute until the failure, on Spherical bearing manufactured by Amsler. Amsler bearing allows deflection in x and y direction. Measuring applied force conducted on Electronic deflectometer Hottenger, type 50, connected to the UPM 60 device. For deflection on x-axis we used five deflectometers along sample length and for y-axis direction three deflectometers, two by the bearings and one in the midsection. Measuring equipment and disposition of measuring points presented on Fig. 4 [19].

Out of six specimens in the same series, two were used to measure dilatations and the test force. Also on the midsection of each specimen were 18 and, on 1/4lenght, 12 measuring tapes. Centrally positioning of the specimen required special attention and multiple observations and adjustments so that midpoints of the end cross-section and bearing match. Imperfections in centric positioning influence on the performance and load bearing capacity of a specimen. This specially emphasized in case where residual stresses have low values so this influence can become dominant. In testing was used five series with different slenderness values. Test results for cyclic loading, as well as maximum deflection values shown on Fig. 5 and Table 6 for specimen U21.

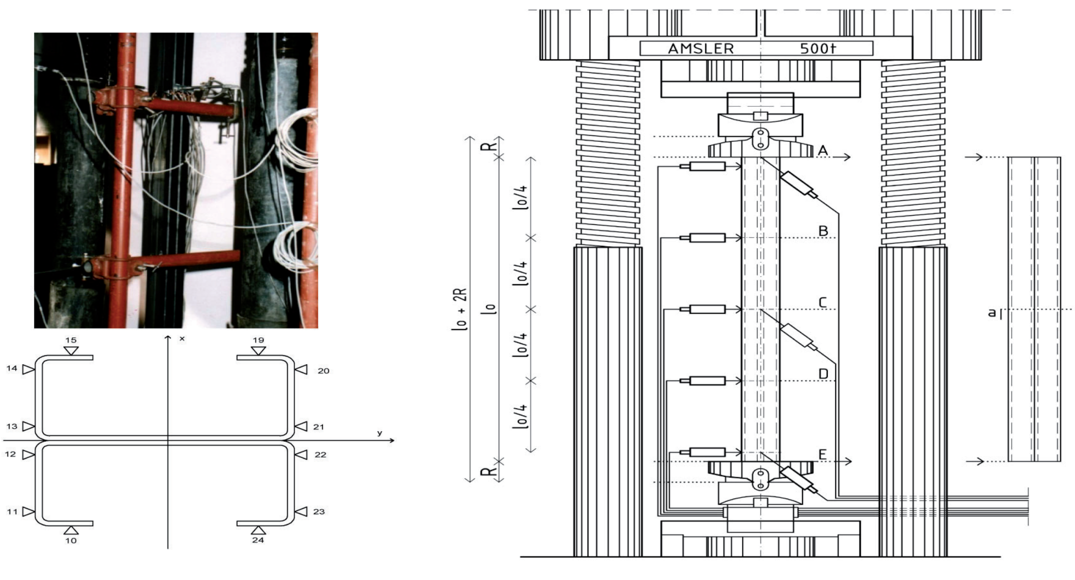

Fig. 4 Measuring equipment and disposition of measuring points

Table 6 Cyclic application of the load, diagrams and deflection table for the specimen U21

Force(kN)	Deflection (mm)						
263.182	1.187	2.375	2.542	2.71	2.238	1.765	0.883
248.035	1.916	3.833	4.541	5.250	4.410	3.570	1.785
245.337	2.137	4.274	5.065	5.855	4.918	3.981	1.991
240.610	2.573	5.147	6.098	7.050	5.922	4.794	2.397
235.462	2.823	5.647	6.691	7.735	6.497	5.260	2.630
Initial deflection	0.16013	0.24325	0.19138	0.1125	0.04263	0.01125	0.03112

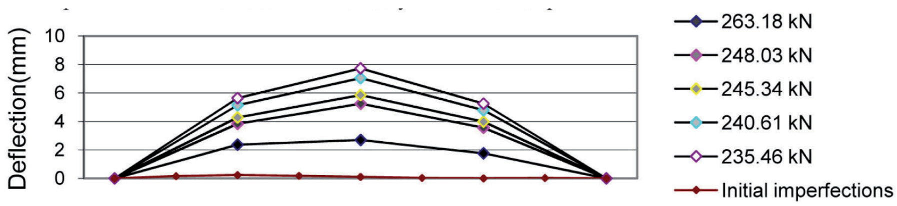

Fig. 5 Initial imperfection and deflection for boundary conditions of specimen U21

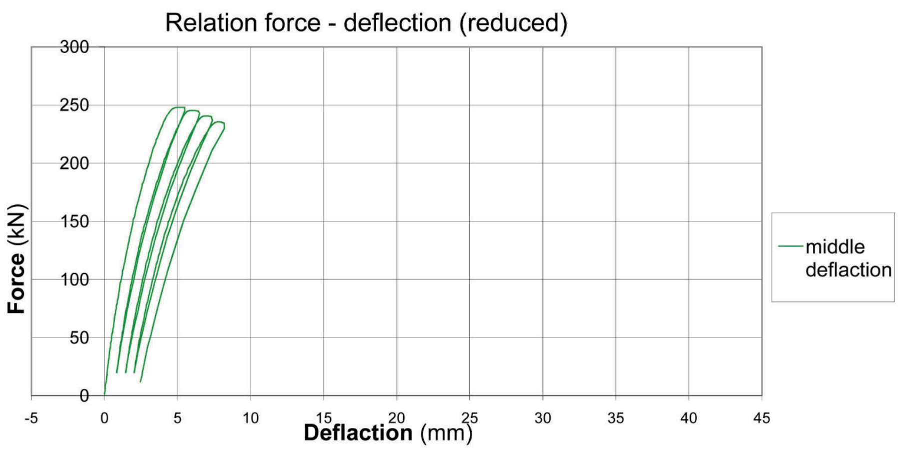

Fig. 6 presents diagram applied force-deflection measured under cyclic load measured on specimen U21.

Along x-axis are marked measured initial imperfections and on the y-axis deflections of cross section under influences of boundary conditions. Measurements were conducted in seven cross sections along longitudinal axis.

3.1 Experimental results for axially compressed members with different slenderness values λ_i

Testing was completed for five series with slenderness values: 50, 70, 90, 110 and 120 and length values: 122.11, 170.95, 219.79, 268.64 and 293.06 cm. Testing results presented on following diagrams reveals relation between maximum deflections and applied forces for cyclic load (Fig. 7 and 8) Measured values are similar on the same profile side while at the opposite side they change orientation under the boundary conditions. Force-deflection diagrams indicate that strains on the compressed side of the section magnified due to the residual stresses caused by manufacturing (cold rolling) processes.

Diagram force-deflection for samples U55 and U64 present maximum deflection and applied forces under cyclic load.

Experimental investigation of the complex member (2 C90 x 45 x 20 x 2.5 mm) under axial load gave us buckling curves that we have compared with European buckling curves from Euro code [5].

Figure 9 and Table 7 present deviations of measured results from European curves (A, B,C,D). From results we can conclude that, in the case when buckling curve calculated according to the yield strength (f_{yl}), obtained in the tensile coupon tests (base sheet coupons), then member design have to include buckling curve “B” for slenderness values λ=70 and λ=90, but for λ=110, λ=120 and λ=50 buckling curve “A”.

3.2 Stub-column test

Stub column test carried out because this production process, known as a cold forming, induces changes in material mechanical properties and residual stresses in the cross section. Yield limits, tensile stress limits, elasticity modulus and elongation percentage acquired by standard tensile coupon tests cannot represent the whole cross section, in other word its

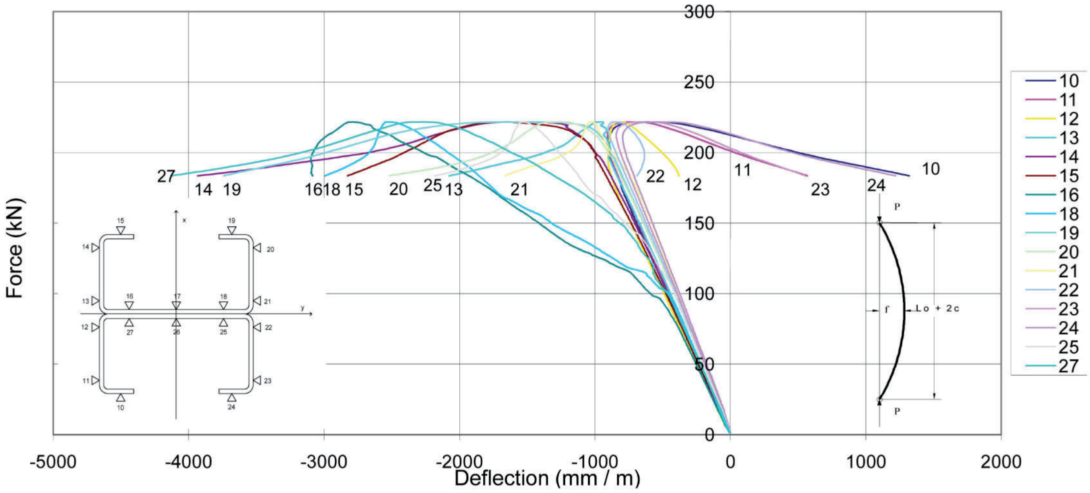

Fig. 7 Diagram of force-deflection relation for specimen U33

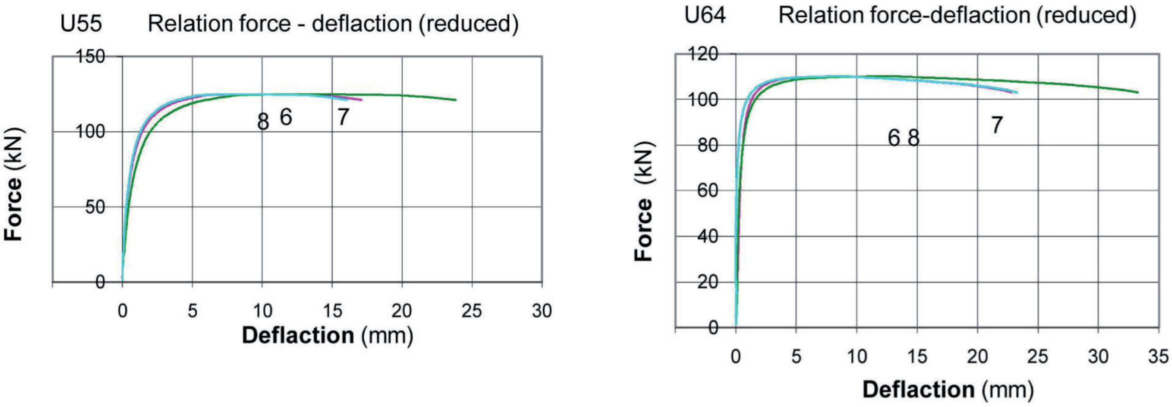

Fig. 8 Diagram force-deflection for samples U55 and U64

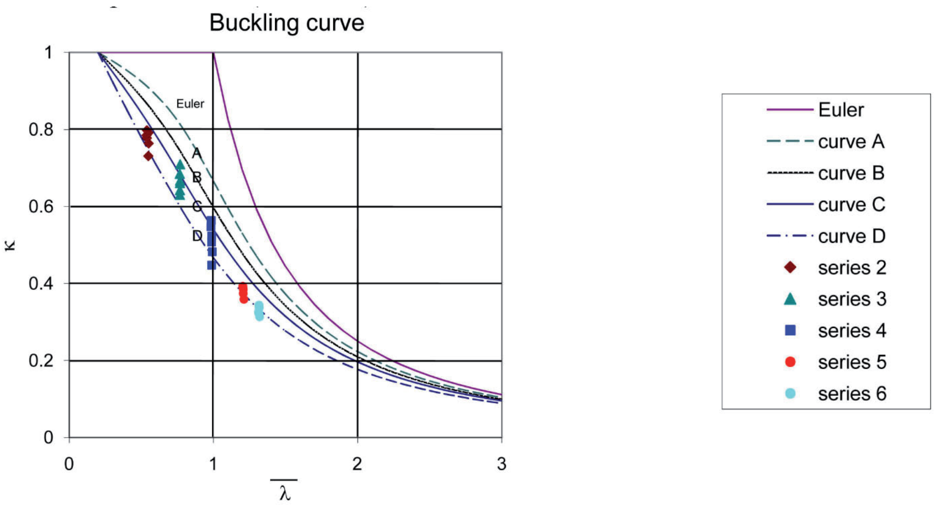

Fig. 9 Buckling curves of complex member obtained experimentally

average stress-strain curve. In this case, average yield limits were determined through compression tests of stub columns.

Stub columns samples investigated in this research were designed so that they are short enough not to include slenderness effects but long enough to include preserve initial magnitude and distribution of the residual stresses. Investigation into behaviour of the stub columns reveals also a local buckling effects, as well as effects of cold forming on the bearing capacity of the column. Height of the stub columns was 366.3 mm in other words 15 λ. Tests were conducted on digitally guided press Amsler 5000 KN. Figure 10 present measurement equipment for measuring stress (f_{yl}) in basic tensile coupons and yield stress (σ_T) in stub column test.

Table 7 Buckling curves of complex member - European curves

Sample	Deviation curve (%)							
		A		B		C		D
U21	-2.21	0.178	-7.75	-5.110	-13.94	-11.031	-24.67	-21.324
U22	1.31		-4.04		-10.02		-20.41	
U23	-2.67		-8.02		-14.01		-24.44	
U24	-0.05		-5.26		-11.09		-21.24	
U25	5.61		0.53		-5.14		-15.01	
U26	-0.91		-6.13		-11.98		-22.17	
U31	7.40	3.975	-1.25	-4.998	-10.41	-14.501	-25.63	-30.295
U32	-2.40		-11.99		-22.14		-39.01	
U33	3.66		-5.36		-14.92		-30.79	
U34	4.67		-4.22		-13.65		-29.33	
U35	9.17		0.70		-8.27		-23.18	
U36	1.33		-7.87		-17.62		-33.82	
U41	22.17	11.029	13.25	0.832	4.10	-9.630	-10.83	-26.695
U42	2.11		-9.11		-20.62		-39.39	
U43	5.31		-5.53		-16.65		-34.80	
U44	8.93		-1.51		-12.22		-29.69	
U45	15.78		6.12		-3.79		-19.95	
U46	11.86		1.76		-8.60		-25.51	
U51	14.27	14.894	5.00	5.695	-4.69	-3.925	-20.69	-19.808
U52	19.37		10.68		1.59		-13.43	
U53	13.17		3.77		-6.05		-22.27	
U54	12.67		3.22		-6.66		-22.97	
U55	13.53		4.17		-5.61		-21.75	
U56	16.36		7.32		-2.12		-17.73	
U61	17.71	16.754	9.41	9.406	0.59	-0.524	-14.11	-15.369
U62	17.79		9.50		0.70		-13.98	
U63	19.90		11.85		3.31		-10.96	
U64	12.58		3.78		-5.56		-21.15	
U65	18.52		10.32		1.62		-12.90	
U66	17.03		5.38		-3.80		-19.12	

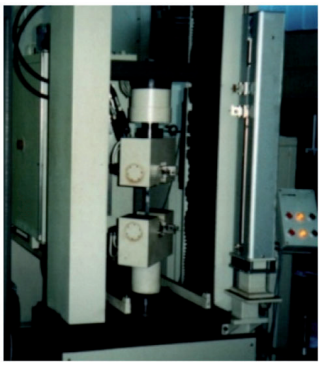

a)

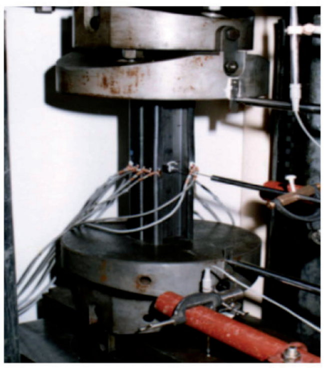

b)

Fig. 10 Measurement equipment for experimental stress testing of basic tensile coupons and stub column

Table 8 Deviations of the experimental results yield stress σ_T and elongation limit of large input material f_{yl}

Stress in basic tensile coupon and in the stub column	U11	U12	U13	U14	U15	U16	Average value
Basic coupon ***fy*l** (Mpa)	272.0	264.0	299.0	281.0	272.0	-	277.6
Stub column **σT** (Mpa)	321.4	323.0	324.7	330.0	326.2	329.0	325.7
Difference **σT - *f*el** (Mpa)	49.4	59.0	25.7	49.0	54.2	-	48.1
Difference (%)	**153.6**	**182.7**	**79.2**	**148.6**	**166.1**	**-**	**147.7**

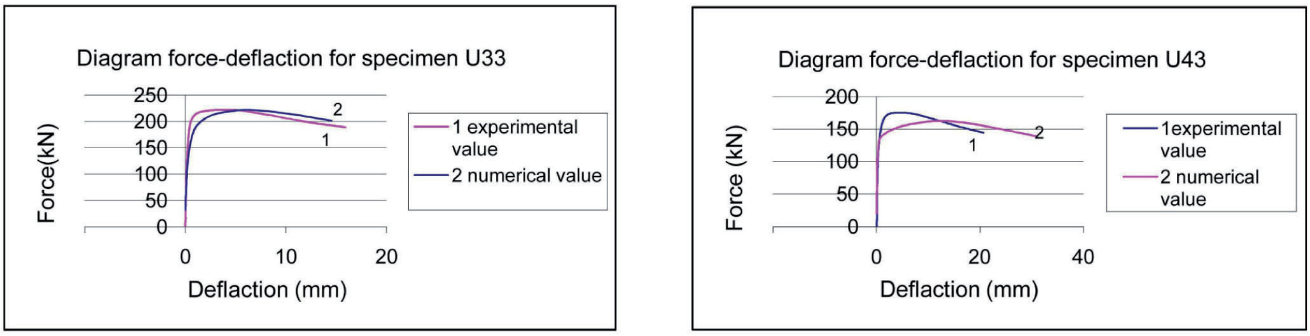

Fig. 11 Diagram force- deflection for specimens U33 and U43 (experimental/numerical value)

Measurements of the force-strain and force-deformation diagrams were electronically monitored. Tests revealed modulus of elasticity and maximal forces as well. In analysis of results we have compared experimentally obtained data for axial bearing capacity of stub columns based on the global yielding and yield limits obtained by standard coupon tests of the input basic steel plate before cold forming (Table 8).

4 Analysis of results obtained by FEM

Numerical analysis of axially compressed complex member was based on finite element method and PAK- software. General beam finite element was used for simulation. It can be also used for linear and nonlinear (geometrical and material nonlinearity) analysis. Cross section is symmetrical according to longitudinal and transversal axis and deformation (buckling) is assumed only in one plane, because only one half (1/2 according to both axis) of the cross section is modelled and calculated [22].

For calculation in numerical analysis, start imperfections defined based on measured values in experimental research. Maximal values of imperfections, in further analysis, varied in order to reveal influence of start imperfections on maximal applied force in member. Deviation member's longitudinal axis from straight line, initial imperfection, defined as a sin function in order to simplify modeling. Results from numerical analysis are presented on diagrams force-deflection. On Fig. 11 are side-by-side presented two force-deflection diagrams, one from experimental and other from numerical analysis.

Diagrams show that average values from both methods are very similar. Numerical results also indicate that complex (2C) member have to be designed according to length, i.e. slenderness for same type of profiles (same forming technology and structural system). For slenderness values λ=70 and λ= 90 members are associated to C buckling curve (Europeans buckling curves), and for λ=110 and λ=120 to buckling curve D. For precise calculation of complex members (2C90x45x20x2.5 mm) in numerical models it is necessary to have real/measured geometrical and structural imperfections.

5 Conclusions

Analysis of structural behavior of cold formed steel sections included behavior of stainless, high grade and carbon steel. Comparing base sheet and complex member characteristics point out that process of cold rolling enhances material characteristics for finished member.

In analysis were used experimental and numerical methods and international designing codes as well. As a result we had three groups of results: experimental, numerical and values predicted by international designing codes, all of them have been compared to each other. Comparisons of results presented in the form of tables and diagrams, enabling overview of most interesting relations.

Matching numerical and experimental results are very similar. Deviation of experimental and numerical curves from international code (Euro code) reveal that in some case international codes are too conservative for cold form steel members. For complex members, with same boundary conditions and production technology, slenderness values have important influence. For particular slenderness values there are recommendations for calculations, in the case when buckling curve is defined according to yield strength (f_{yl}) obtained in tensile coupon test (coupons from base sheet) :

- λ=70 and λ=90 for calculation is recommended to use European curve B
- λ=110, λ=120 and λ=50 for calculation is recommended to use European curve A

For lower slenderness values, additional research has to be performed with aim to define their buckling curve. Suggestion is to make calculations associated with the buckling curve A, for safety reasons.

References

[1] Narayanan, S., Mahendran, M. "Ultimate capacity of innovative cold-formed steel columns." *Journal of Constructional Steel Research*. 59(4), pp. 489-508. 2003. DOI: 10.1016/S0143-974X(02)00039-1

[2] Ellobody, E., Young, B. "Structural performance of cold-formed high strength stainless steel columns." *Journal of Constructional Steel Research*. 61(12), pp. 1631-1649. 2005. DOI: 10.1016/j.jcsr.2005.05.001

[3] "Specification for the design of cold-formed stainless steel structural members." ANSI/ASCE-8-90, American Society of Civil Engineers (ASCE), 1991.

[4] "Cold-formed stainless steel structures." AS/NZS 4673:2001, Australian/New Zealand Standard, Sydney, 2001.

[5] Eurocode 3 (EC3): European Committee for Standardization. EN 1993-1-4:2006. Design of steel structures - Part 1-4: General rules - Supplementary rules for stainless steels. European Committee for Standardization.

[6] Eurocode 3 (EC3): European Committee for Standardization. EN 1993-1-1:2005. Design of steel structures - Part 1-1: General rules and rules for buildings n of steel structure. European Committee for Standardization.

[7] Eurocode 3 (EC3): European Committee for Standardization.. EN 1993-1-8:2005. Design of steel structure – part 1-8: Design of joints, European Committee for Standardization.

[8] Gao, L., Sun, H., Jin, F., Fan, H. "Load-carrying capacity of high-strength steel box-section I: Stub columns." *Journal of Constructional Steel Research*. 65(4), pp. 915-924. 2009. DOI: 10.1016/j.jcsr.2008.07.002

[9] Young, B., Lui, W. M. "Test of cold high strength stainless steel compression members." *Thin-Walled Structures*. 44(2), pp. 224-234. 2006. DOI: 10.1016/j.tws.2006.01.006

[10] Ellobody, E. "Buckling analysis of high strength stainless steel stiffened and unstiffened slender hollow Section columns." *Journal of Constructional Steel Research*. 83(2), pp. 145-155. 2007. DOI: 10.1016/j.jcsr.2006.04.007

[11] Sedlacek, G., Müller, C. "The European standard family and its basis." *Journal of Constructional Steel Research*. 62(11), pp. 1047-1059. 2006. DOI: 10.1016/j.jcsr.2006.06.027

[12] Liu, Y., Young, B. "Buckling of stainless steel square hallow section compression members." *Journal of Constructional Steel Research*. 59(2), pp. 165-177. 2003. DOI: 10.1016/S0143-974X(02)00031-7

[13] Young, B., Lui, W. M. "Test of cold high strength stainless steel compression members." *Thin-Walled Structures*. 44(2). pp. 224-234. 2006. DOI: 10.1016/j.tws.2006.01.006

[14] Goggins, J. M., Broderick, B. M., Elghazouli, A. Y., Lucas, A. S. "Behavior of tubular steel members under cyclic axial loading." *Journal of Constructional Steel Research*. 62(1-2), pp. 121-131. 2006. DOI: 10.1016/j.jcsr.2005.04.012

[15] Cruise, R. B., Gardner, L. "Residual stress analysis of structural stainless steel section." *Journal of Constructional Steel Research*. 64(3), pp. 325-366. 2008. DOI: 10.1016/j.jcsr.2007.08.001

[16] Cruise, R. B., Gardner, L. "Strength enhancements induced during cold forming of stainless steel sections." *Journal of Constructional Steel Research*. 64(11), pp. 1310-1316. 2008. DOI: 10.1016/j.jcsr.2008.04.014

[17] Gardner, L., Nethercot, D. A. "Experiments on stainless steel hollow sections-Part 1: Material and cross-sectional behaviour." *Journal of Constructional Steel Research*. 60(9), pp. 1291-1318. 2004. DOI: 10.1016/j.jcsr.2003.11.006

[18] Besević, M., Kukaras, D. "Analysis of structural changes in cold formed steel profiles occurred as a technology." *Journal of Materials in Civil Engineering*. 23(9), pp. 1369-1375. 2011. DOI: 10.1061/(ASCE)MT.1943-5533.0000311

[19] Besević M. "Contribution to analysis of axially compressed cold formed steel members." Doctoral Thesis. Belgrade, Serbia, p.166. 1999.

[20] Jandera, M., Gardner, L., Machacek J. "Residual stresses in cold-rolled stainless steel hollow section." *Journal of Constructional Steel Research*. 64(1), pp. 1255-1263. 2008. DOI: 10.1016/j.jcsr.2008.07.022

[21] Besević, M. "Experimental investigation of residual stresses in cold formed steel sections." *Steel and Composite Structures*. 12(6), pp. 465-489. 2012. DOI: 10.12989/scs.2012.12.6.465

[22] Kojić, M., Slavković, R., Živković, M., Grujić, N. "Program for Structural nonlinear Analysis." - PAK, 1992. , Faculty of Mechanical Engineering in Kragujevac, Serbia, 1992.